C.5

SANDIA REPORT

SAND96–0519 • UC–703
Unlimited Release
Printed March 1996

HALFTON—A High-Explosive Containment Experiment in Partially Saturated Tuff

Carl W. Smith

Prepared by
Sandia National Laboratories
Albuquerque, New Mexico 87185 and Livermore, California 94550
for the United States Department of Energy
under Contract DE-AC04-94AL85000

Issued by Sandia National Laboratories, operated for the United States Department of Energy by Sandia Corporation.

Available to DOE and DOE contractors from
Office of Scientific and Technical Information
PO Box 62
Oak Ridge, TN 37831

Prices available from (615) 576-8401, FTS 626-8401

Available to the public from
National Technical Information Service
US Department of Commerce
5285 Port Royal Rd
Springfield, VA 22161

NTIS price codes
Printed copy: A03
Microfiche copy: A01

SAND 96-0519
Unlimited Release
Printed April 1996

Distribution
Category UC–703

HALFTON – A High-Explosive Containment Experiment in Partially Saturated Tuff

Carl W. Smith
Applied Technology Department
Sandia National Laboratories
Albuquerque, NM 87185

Abstract

The HALFTON experiment explored the phenomena of high explosive detonations in 90% water-saturated tuff rock. The explosive source was a 453 kg TNT sphere which was grouted in a drift in G Tunnel, Nevada Test Site. Active gages measured stresses and motions in the range of 1.3 to 5.3 cavity radii and showed a peak stress decay as range raised to the -2.77 power. Additional stress gages were fielded to investigate the gage inclusion problem.

Contents

Figures

Tables

HALFTON – A High-Explosive Containment

Experiment in Partially Saturated Tuff

Preface

Ten years after HALFTON was designed, fielded, fired, and described in a rough draft, we find time to review the draft and decide its "fate". The 1985 memo describing the design of the experiment stated, "a major juggling of the different combinations of grout and (gage emplacement) geometries have been performed to maximize the (data) return while holding the gages to a reasonable number." The assessment in hindsight is that too many questions were asked. Also, fielding problems compromised objectives and added more variables.

Ten years later we find that the HALFTON data have been cited by a number of authors. Of interest is the clearly measured attenuation of peak stress in the 90% saturated tuff. Attenuation in saturated tuff is well known from numerous measurements on nuclear and high explosive events; however, few measurements exist in the drier tuffs with known saturation. There is a major change of attenuation between these two saturations. Question: why was this of interest? Answer: containment of underground nuclear events. For some types of events containment was enhanced by a slow decay of stress with range. For other events designers desired a rapid decay.

HALFTON also addressed gage inclusion effects. Some measurements confirmed calculational modeling of the gage and its emplacement geometry. Other measurements showed significant departure from modeling work. (Measurements on a subsequent experiment confirmed this discrepancy.) Although incomplete, the work contributed to the understanding of gage inclusion effects. Nuclear testing has ended; however, these effects are still present in stress measurements made on high-explosive, field experiments.

Introduction

The HALFTON event was one of a series of high-explosive experiments designed to explore the interaction of an explosion with volcanic tuffs. Of particular interest were the effects that led to the successful "containing" of underground nuclear events, that is, containing the radioactive debris and cavity pressure within the cavity. Also of interest to the nuclear test community is wave propagation phenomenology in tuffs of varying water saturation.

It is currently believed that in tuff-type geologies, the "containing effect" is the so-called residual stress field. This is a zone of compressive stress in the material about the cavity that remains after the dynamic effects of the explosion pass. If the "hoop" component of this stress field is larger than the cavity pressure, it will prevent the cavity pressure from driving fractures through the cavity wall

and, thus, to the nearest free surface.

We are using the following approach:

– Prove that the residual stress field exist

– Explore the amplitude, extent and decay of the stress field with measurements

– Model the phenomena with computer calculations

With successful achievement of these tasks, one can then attempt to calculate and predict the residual stress field in nonspherical geometries; for example, those generated by experiment hardware such as a line-of-sight pipe or in an unusual geologic setting.

In the PUFF TOO experiment[1], we measured the pressures necessary to drive fractures in the presence of the residual stress field. Compared with nearby, pre-event hydraulic fracture work, significantly larger pressures were necessary to drive fractures near the explosively formed cavity. Data from active stress-time gages used on that and other events have also shown evidence of the residual stress field and its decay. Compromising the measurements are two problems:

– Surviving the spherical divergent motion fields by the gage packages and their electrical conductors.

– Relating the measured stress in the drill hole and coupling grout to the free-field stress – the so-called inclusion problem.

On HALFTON we tackled and made progress on these two problems.

We sited HALFTON in a partially saturated (90%) tuff unit; most previous experiments were sited in nearly saturated (98%) tuff. The reasons were twofold. There are limited measurements in tuff at lower saturations; yet stress attenuation, other wave propagation effects, and residual stress in the drier material is of strong interest. Second, calculations and material models have evolved to treat nearly saturated tuffs. By changing the water content, we can test the material models, that is, do they have predictive capabilities for a material other than the nearly saturated tuffs.

This report describes a field experiment using high explosive to obtain stress and motion data in a partially saturated tuff and to obtain data on gage inclusion effects. In the following sections we describe:

– the geological setting and its material properties
– the details of the experiment
– the fielded gages
– the dynamic measurements
– the inclusion experiments
– the mineback

Location and Geology

We fielded HALFTON in a partially saturated tuff unit in G-Tunnel, locate in Rainier Mesa, at the Nevada Test Site (NTS). The 453 kg (1000 pound) of high explosive was located in a drift excavated from the end of the mineback drift of the DM 1 and 2 model experiments. (From this previous work, we know that this site has a lower water saturation than usual.) The geology was explored with three drill holes; they gave the thickness of the bed and its dip and strike. Cores from these holes were tested and showed some strength variation from the top to the bottom of the bed. To conduct the experiment in the same strength material we located the charge and gages at the same height above the dipping, lower boundary of the bed. The 4G tunnel bed is about 4.5 meters thick and consists of zeolitized, peralkaline ashfall tuff.

Material Properties

In addition to the tests on cores to explore the 4G tunnel bed, we sent four samples from the gage holes to Holmes and Narver (H&N) Material Testing Laboratory at NTS. Data from their tests are given in Table 1.

Table 1. Material Properties from H&N Tests

Property	Average Value
Densities (Mg/m^3)	
Natural	1.77
Dry	1.39
Grain	2.46
Calculated porosity	43.3%
Saturation	86.9%
Unconfined crush strength	19.5 MPa
Modulus of elasticity	3.87×10^3 MPa
Poisson's ratio	0.12
Sonic pulse compressive speed*	1.79 km/s
Sonic pulse shear speed*	0.946 km/s

* Data from samples from geology hole GH3

Eleven samples were sent to TerraTek Research (Salt Lake City) for material properties tests and uniaxial strain tests to 4 kbar. Their results are described in two reports[2,3]. Table 2 gives averaged material properties values from the 11 samples. Figure 1, from reference 3, shows a representative uniaxial test. To simulate the in-situ loading on the rock, TerraTek hydrostatically loaded the samples to 6.9 MPa and allowed them to creep. Then they proceeded with the uniaxial strain test; the beginning of the uniaxial test is marked.

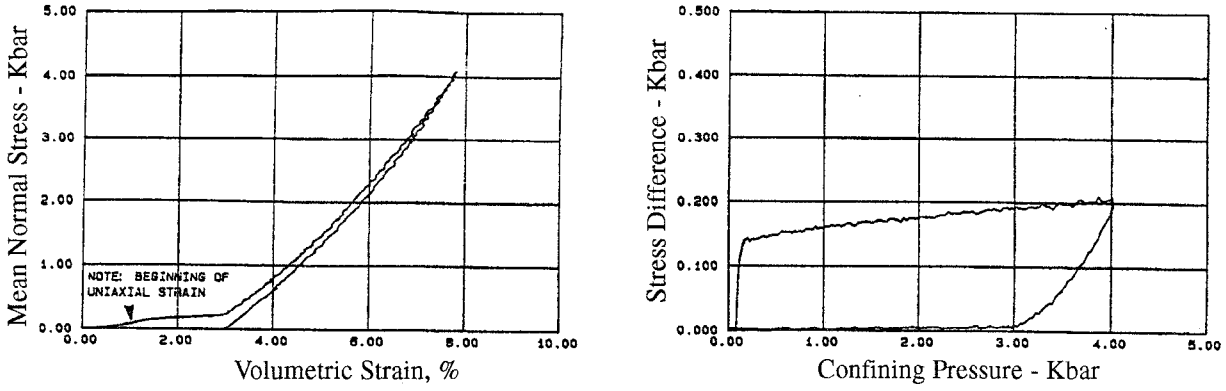

Figure 1. Typical Uniaxial Strain Response of HALFTON Tuff

Table 2. Material Properties from TerraTek Tests

Property	Average Value
Densities (Mg/m^3)	
Natural	1.79
Dry	1.39
Grain	2.45
Moisture content (wt%)	22.2%
Porosity	43.2%
Saturation	92.0%
Air voids	3.5%
Ultrasonic compressive speed	2.12 km/s
Ultrasonic shear speed	1.06 km/s

In addition, TerraTek performed a series of uniaxial strain tests on the GCRM grout. This grout is a field-cast version of SRI International's 2C4 grout. As measured by TerraTek, the compression and shear properties of the GCRM grout are a closer match to the properties of HALFTON tuff than a normal rock matching grout. As described by Swan[4], matching the pressure versus volume response, that is, the compressibility of the grout and tuff, minimizes the gage inclusion effect.

Experiment Details

Figure 2 shows a plan view of the experiment. The charge insertion drift was located at the end of the DM1 and DM2 mineback drift and was mined using a drill and blast technique. Note the work point (WP) location at the end of this drift. Figure 3 shows the TNT charge fitted into a hand chipped alcove at the end of the drift. This technique minimized the amount of grout between the charge and the gage array. The white plastic pipe extending from the charge was used to hold spiral cavity pressure pipe fielded by Science and Enginering Associates. The plywood box, in the lower right with the heavy cables housed LLNL's gas sampling experiment. This drift was stemmed with

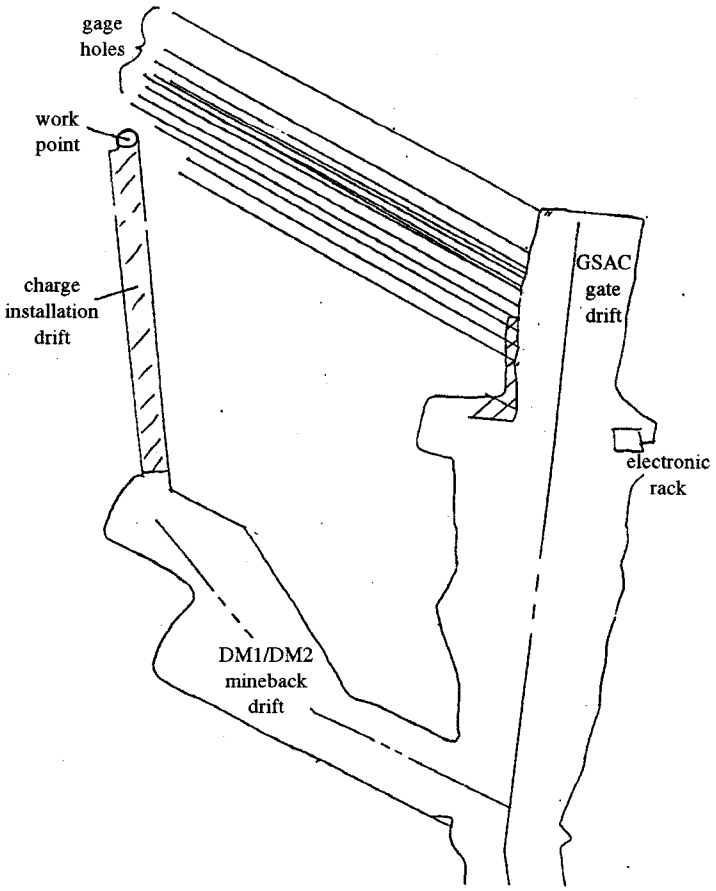

Figure 2. Plan View of HALFTON

a high strength groutcrete (HLHSGC[CC]). On shot day, samples of this grout pour showed an unconfined compressive strength of 43.4 MPa (6300 lb/in^2).

The HE charge consisted of a cast 453 kg (1000 lb) TNT sphere 81.9 cm (32.25 inches) in diameter that contained a 25.4 cm (10 inch) diameter penolite booster. The charge was center detonated with an exploding bridgewire.

Gage holes were "collared" (started) in the GSAC gate test drift; most of them extended past the point of tangency of the hole and a spherical wave from the charge – see Figure 2. With these so-called tangential holes, the paddle-type gages were loaded "face on." Two radial holes (15 and 16) were also used; these contained Toadstool stress gages; this set of gages comprised one of the gage inclusion experiments. To exclude air bubbles in the grouting process, all holes were inclined at least 5 degrees below the horizontal. Drill holes were oriented so that the gages could be located at tangency points and in the center of the dipping, geologic bed.

Gage power supplies and calibration equipment were located in an electronic rack located in the gate test drift. Electrical cables carried the signals to the underground signal alcove about 274 m (900 ft.) from the WP. Signal conditioning and recording equipment were located in the alcove. During the shot this equipment was operated from outside the tunnel complex.

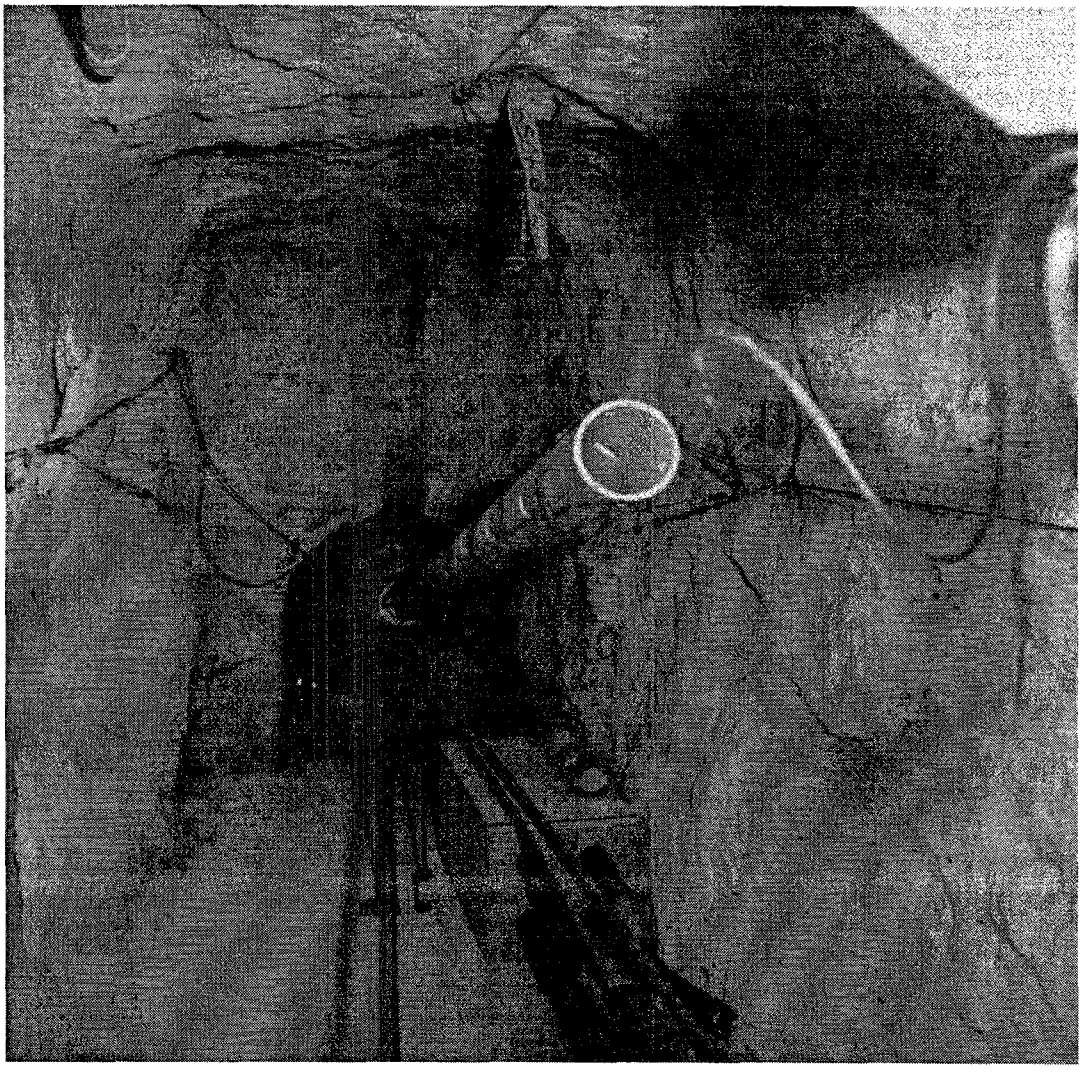

Figure 3. View along Installation Drift

Gages were recorded on two high-speed FM tape recorders. High-frequency signals were recorded on wide-band equipment; lower-frequency signals were multiplexed. Additional channels – at lower gains – provided redundant recording. These analog data were subsequently low-pass filtered and digitized. The multiplex recorded data showed poor signal to noise ratios; some of these channels required filtering at frequencies as low as 1 kHz. In addition to the high-speed recording, we used a minicomputer (Hewlett Packard 9845) to obtain late-time stress data.

Gages

Many of the gages fielded on this experiment were fluid-coupled ytterbium paddles. The gage shown in the lower portion of Figure 4, and marked 6BYB, is a typical example. Dimensions of the gage body are 30.5 cm long, 7.6 cm high, and 0.94 cm thick. The paddle is made of layers of fiberglass board and epoxy. The piezoresistive ytterbium grid floats in a thin fluid cell. The cell

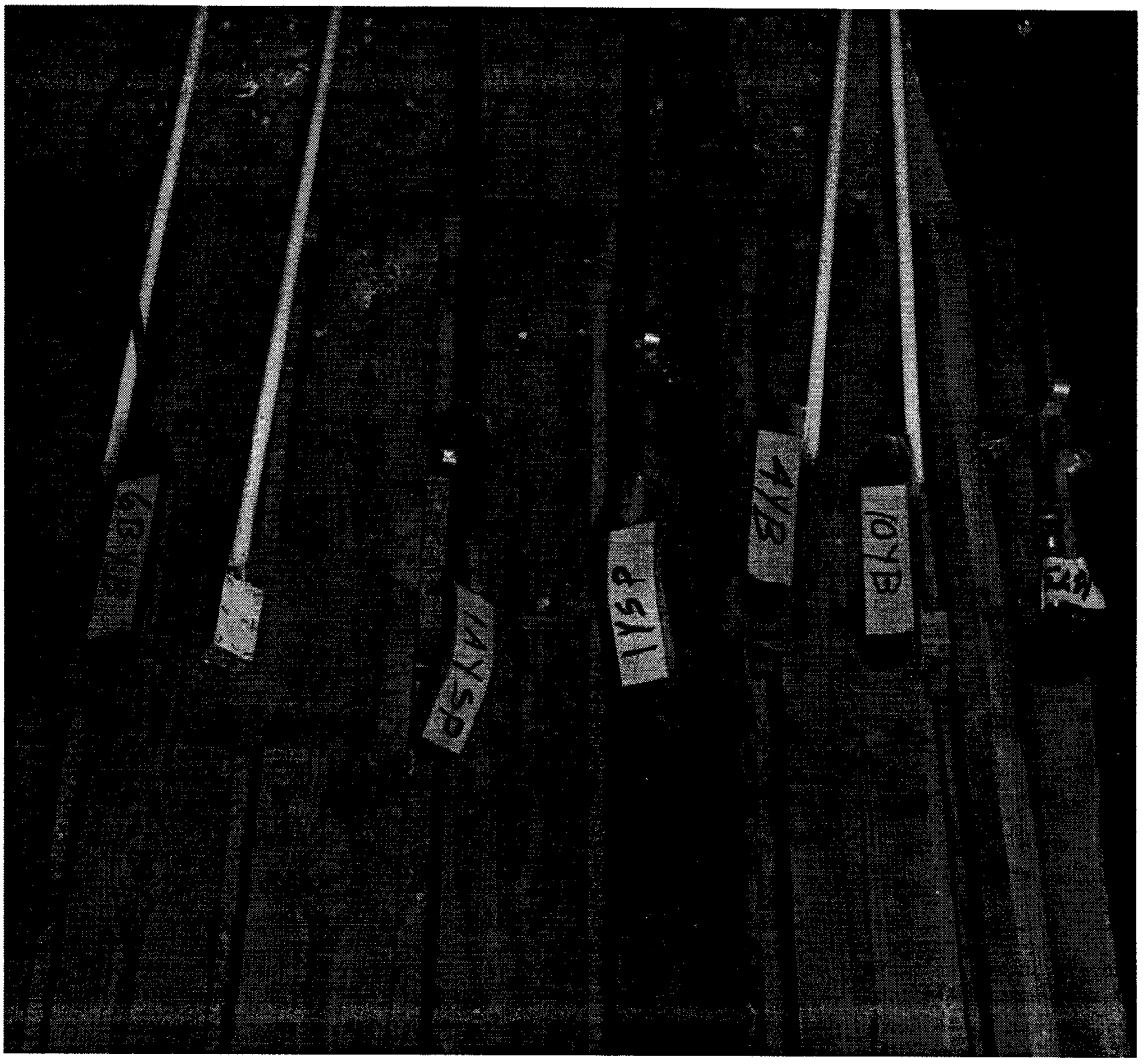

Figure 4. Stress and Acceleration Gage Packages

is approximately rectangular with dimensions: 6.4 cm long, 5.1 cm high, and 0.51 cm thick. The purpose of the fluid-coupling is to prevent the lateral strain associated with the spherically divergent flow field from being transmitted to the ytterbium grid. With this scheme the ytterbium grid measures the pressure in the glycerin fluid. On the RS15 experiment, we studied the relation between this dynamic pressure and the radial stress. A grid was sandwiched between two pieces of fiberglass board; this is the typical arrangement for a radial stress gage. In the same fiberglass composite were three fluid-filled cells. Each contained a ytterbium grid; the coupling fluids were a

relatively compressible silicon fluid (Dow Corning DC10), glycerin, and mercury. The peaks from the fluid-coupled grids bracketed the 1.11 kbar peak shown by the solid-coupled radial stress grid; the grid in the mercury cell showed a 7% greater peak, the glycerin-coupled grid showed a 10% lower peak, and the silicon oil cell showed a 19% lower peak. On unloading the fluid-coupled grids showed the expected residual amplitudes; the solid-coupled grid unloaded to a level below zero stress. This was expected since the lateral strain associated with divergent flow was coupled into the grid, and we know that ytterbium decreases in resistance when subjected to lateral strain. These strain effects are comparable in amplitude to the residual stresses we wish to measure.

With the fluid-coupling technique, we can eliminate the lateral strain effect on the ytterbium grid; however, for gages close to the WP, these strains will break electrical cables. On this experiment we fielded two "spatula" gages in an attempt to minimize this problem. Figure 5 shows the arrangement of the spatula gage, its grouted hole, and the work point. Here we are attempting to balance the lateral tensile strain on the cable against the radial compressive strain. We are using a technique developed by Hartenbaum[5]. With straight holes, one can match these two strains only

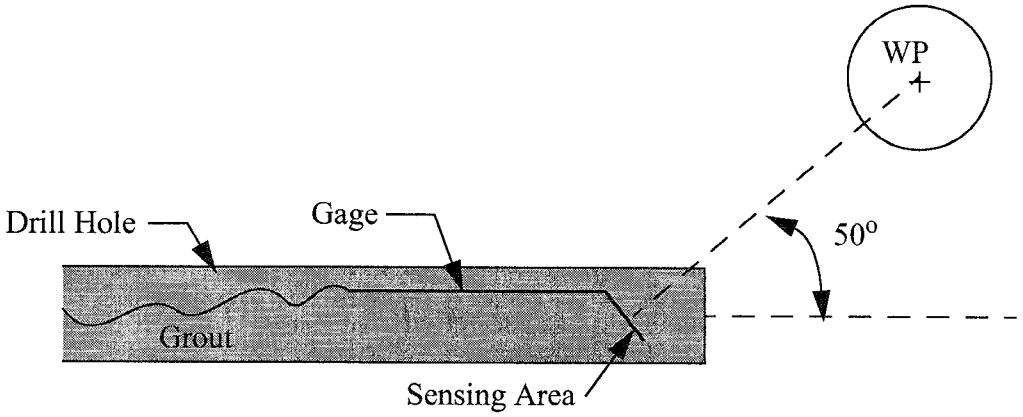

Figure 5. Spatula Gage – Installation Geometry

at one range. We match them at gage location, thus the gage holding fixture and cable farther from the work point were put in compression. The disadvantage of this technique is that the gage may see some stress effects from the presence of the end of the hole. These are minimized by using a grout whose compressibility matches that of the rock host. Also, we are close enough to the charge that both the grout and rock plastically yield; this also minimizes mismatches. A minor disadvantage is that the gage is not centered in a circular hole; thus a calculational modeling of the configuration is no longer two dimensional. The two spatula gages are shown in Figure 4; they are marked 1YSP and 1AYSP.

The other variation on the typical ytterbium paddles consists of building a thinner package – 4.8 mm versus 9.5 mm. These gages – 10YB and 4YB – were slated for 1.5 cm wide slots to be cut at the end of drill holes. We felt we needed a larger air gap around the gage to allow grout to flow into slot. Because of problems encountered in cutting the slot at the end of the 15.2 cm (50 feet) drill hole, we only achieved one slot (10YB); gage 4YB was centered in a 15.2 cm (6 inch) diameter drill hole.

Two Pancake gages were fielded on this event. This gage consists of a thin, fluid-filled cell formed by two circular aluminum plates. The pressure in the cell is measured by a commercial pressure sensor housed in a cylindrical section attached to the aluminum plates. Figure 6 shows these two gages before installation. The one closest to the centering fixture was loaded face-on, thus it should sense radial stress; the other was loaded edge-on and should respond to the hoop stress. The thrust of the latter is gage development. The intent of the radial stress measurement with the Pancake gage was to permit a comparison with the ytterbium gages. (This is an accuracy issue, that is, to see if there is a systematic bias to the ytterbium measurements.)

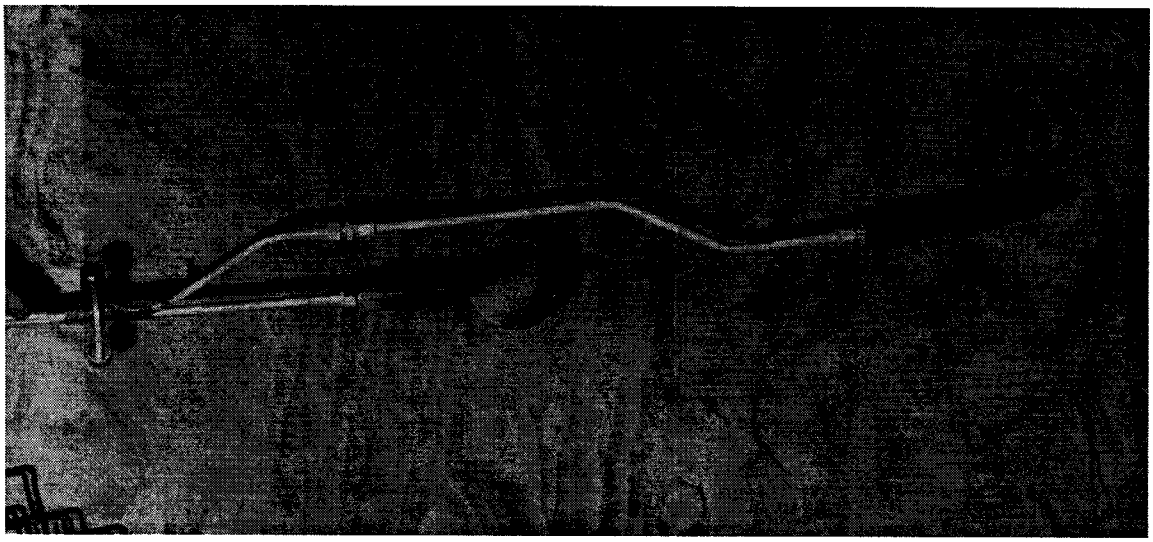

Figure 6. Pancake Gages to Measure Radial and Hoop Stress Components

Toadstool gages are similar to the pancake-gages; the difference is that the two aluminum disks are mounted perpendicular to the cylindrical section that houses the pressure transducer. One of these gages (16TS) – the top one in Figure 4 – was centered and grouted in a 15.2 cm (6 inch) diameter, radial drill hole. A companion radial hole contained an aluminum-loaded epoxy (REN) cylinder containing two of these Toadstool gages. The 10.2 cm (4 inch) cylinder was centered and grouted in the number 15 hole. The radially oriented, epoxy cylinder package scheme is the standard technique we use for fielding gages on nuclear events. Pacifica Technology[4] has performed a series of inclusion calculations to examine the relation between stress measured in the epoxy cylinder and the stress in the free field. We wanted data from these three Toadstool gages to compare with the calculations.

Lithium niobate gages represent a different type of stress gage from the fluid-cell gages in that they are crystalline, piezoelectric transducers. Again, we are addressing the gage accuracy issue. Previous measurements with lithium niobate[1] have shown greater stress amplitudes than from ytterbium gages. On this experiment we fielded two Z-cut, lithium niobate, component gages. Like the pancake gages, we turned one so that it would be loaded edge-on.

Five accelerometer packages were fielded on this event. Each package consists of a piezoresistive

accelerometer (Endevco, Model 2264) mounted in an aluminum housing. The second gage from the bottom in Figure 4 is the 14AC accelerometer package. The remaining four packages were attached to ytterbium paddles. Previous experiments with this type gage have produced credible data. Existing, but limited, data suggests that acceleration decays rapidly with range in unsaturated tuff. Thus, our problem on this event was to estimate peak accelerations, select gages, and set recording band edges that would not over, nor under, range the peak amplitudes.

Table 3 lists the gages, their ranges to the WP, the type of grout, the age of the grout, and the gage description. (YBFC denotes a fluid-coupled ytterbium paddle.)

Table 3. Gages, Ranges, Grout Type and Age

Gage	Range (meter)	Grout	Age (days)	Gage Description
1YSP	1.41	GCRM	72	YBFC Spatula Shape
1AYSP	2.08	GCRM	72	YBFC Spatula Shape
2YB	1.37	GCRM	72	YBFC
3YB/3AC	1.89	GCRM	72	YBFC and Accelerometer
4YB	1.96	GCRM	9	YBFC Thin Paddle in a 15.2 cm (6 inch) hole
5YB/5AC	2.52	GCRM	72	YBFC and Accelerometer
6YB	2.38	HPNS2	78	YBFC Plus Nickel Grid
7PCR/7PCT	2.65	GCRM	72	Radial and Hoop Pancake
8YB/8AC	3.08	GCRM	72	YBFC and Accelerometer
10YB	3.12	HLNCC	9	YBFC Thin Paddle in Slot
11LNR/11LNT	3.51	GCRM	72	Radial and Hoop Lithium Niobate
12YB/12AC	3.95	GCRM	72	YBFC and Accelerometer
13YB	4.03	HPNS2	73	YBFC
14AC	5.68	GCRM	72	Accelerometer
15TSF	2.75	HPNS2	78	Front Toadstools in REN Cylinder
15TSC	3.23	HPNS2	78	Center Toadstool in REN Cylinder
16TS	2.70	HPNS2	78	Bare Toadstool in 15.2 cm (6 inch) Radial Hole

The newly developed GCRM grout was used to grout the gages that would define stress wave propagation in the partially saturated tuff. The 6YB and 13YB gages were grouted with HPNS2. Its pressure versus volume strain curve is different from GCRM. Calculational analysis[4] suggested that we should see reduced peak stress in this softer grout. Holes 15 and 16 were also grouted with HPNS2 for this is the usual grout used in fielding the epoxy cylinder gages in radial holes. The last notable item in the table is the two gages with the nine day-old grout – 4YB and 10 YB. These two thin paddles were scheduled for slots at the expected 2 and 0.5 kilobar levels. We encountered significant development problems with the modified chain saw that was used to cut the slots. Meanwhile the grout for the rest of the gages was aging. In cutting one slot we wore out a portion of the tool and decided to proceed with the single slot.

Gage Measurements

All 29 of the gages fielded on HALFTON produced records. Some were quite noisy due to the inherent noise levels in multiplex equipment and conservative setting of some band edges. The accelerometer records were the noisiest. Because of the poorly known attenuation rate of peak acceleration in partially saturated tuffs, we conservatively set recording band edges based on data from saturated tuff. In some cases the data competed with the inherent noise in the multiplex recording equipment.

To give an overview of the data, we present a table of peak stresses and arrival times followed by plots of these quantities versus ranges. Subsequently, we display and discuss gage waveforms. Table 4 shows gage ranges, times of arrival, and peak values. The time of arrival data is for the main wave; gages installed with GCRM show small precursors to the main wave.

Table 4. Stress Gage Measurements: Times of Arrivals, Peaks and Residual Values

Gage	Range (meter)	Time of Arrival (millisecond)	Peak (kbar)	Residual Level (kbar)
lYSP	1.41	0.49	3.2	0.05
1AYSP	2.08	1.05	1.04	0.35
2YB	1.37	0.52	3.6	-
3YB	1.89	0.93	1.32	-
4YB	1.96	0.87	1.25	-
5YB	2.52	1.38	0.71	0.20
6YB	2.38	1.01	0.93	-
7PCR	2.65	1.69	0.49	0.1
7PCT	2.65	1.61	0.075	0.025
8YB	3.08	1.86	0.39	0.06
l0YB	3.12	1.40	0.26	0.02
11LNR	3.51	1.62	0.46	0.03
11LNT	3.51	1.52	0.04	0
12YB	3.95	2.95	0.196	0.02
13YB	4.03	1.82	0.16	0.04
15TSF	2.75	1.18	0.86	0.31
15TSC	3.23	1.39	0.94	0.4
16TS	2.70	1.15	--	0.14

Figure 7 shows times of main energy arrival versus range. Some scatter is seen in this data. The late arrivals are associated with gages grouted with GCRM; consistent arrivals are shown by gages grouted with HPNS2. A least squares fit to the HPNS2 data is shown; its slope is the wave speed of 1976 m/sec (6483 ft./sec). As mentioned above, there are often precursors seen on the gages grouted with GCRM; the precursors, 5YB for example, are sometimes close to the least squares fit. The time discrepancy between the main energy arrival for gages grouted with GCRM and the gages grouted with HPNS2 increases with range. The notably late gage is 12YB; here the precursor arrives about a millisecond before the arrival shown by the companion, HPNS2 grouted, gage. A

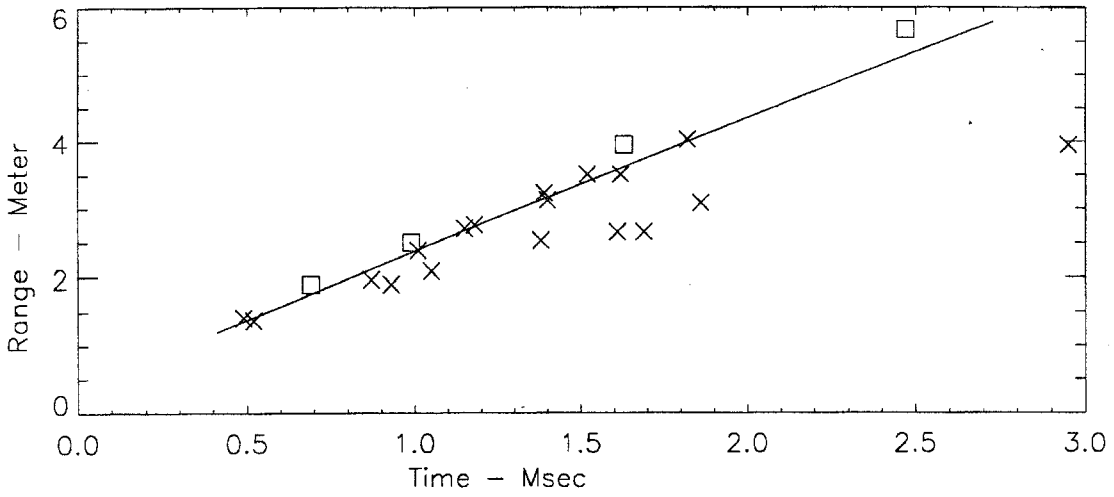

Figure 7. Time of Arrival versus Range

possible explanation of these late arrivals is that the 90% saturated host rock absorbed water from the grout and left an annulus of weak grout material. Motion associated with particle velocity was required to compress this annulus before the main energy was felt by the gage package. With increasing range, peak particle velocity decreases and thus longer times were required before the gage showed the arrival of the main energy. An alternate explanation is that the GCRM grout may have shrunk slightly leaving a gap at the grout-tuff interface. As is usually observed, accelerometers show arrivals slightly earlier than stress gages. Time of arrivals from four accelerometers – the squares in Figure 7 – are consistent with range and show a wave speed of 2137 m/sec (7011 ft./sec). Interestingly, the accelerometer attached to the 12YB stress gage showed an arrival consistent with gages grouted with HPNS2. Some acceleration waveforms may have been affected by the GCRM grout.

Figure 8 shows peak stress values versus range. The stress attenuation line is a least squares fit of the ytterbium paddle gages fielded in drill holes (1YSP, 1AYSP, 2YB, 3YB, 4YB, 5YB, 6YB, 8YB, 12YB, and 13YB); deviations from the line for these gages are small. The slope is -2.77. Other gages lie off the line. The lithium niobate radial stress gage (11LNR) shows a peak 1.7 times the value predicted from the ytterbium paddles. Ytterbium paddle 10YB was fielded in a slot; its peak is 70% of the fitted line. We discuss this value in the inclusion section. The peak shown by the pancake gage (7PCR) is also low; its peak is 82% of the fitted line. Another peak departure from the ytterbium paddle line is shown by the pancake gage 7PCR. Our only comment is that it is a different type gage. Lastly, we see that the 15TS gages show peaks well above the line. These were fielded in an epoxy cylinder and are discussed in the inclusion section.

In the next series of figures we show the stress waveforms and make some comparisons. Figure 9 shows waveforms from the two spatula gages (1YSP and 1AYSP) and from a paddle gage (3YB). Both 3YB and 1YSP show small precursors. Although the peaks from gages 3YB and 1AYSP are similar, the unloading portion of the waves differ. This may reflect the gage and hole geometry, i.e., the bent spatula gage near the end of the drill hole versus the straight paddle in a hole. Gage 3YB broke near 3.2 msec; at 10.5 msec the trace returned for 2 msec and showed a level of about 0.2 kbar. Spatula gages 1YSP and 1AYSP survived the early dynamic motions; their waveforms

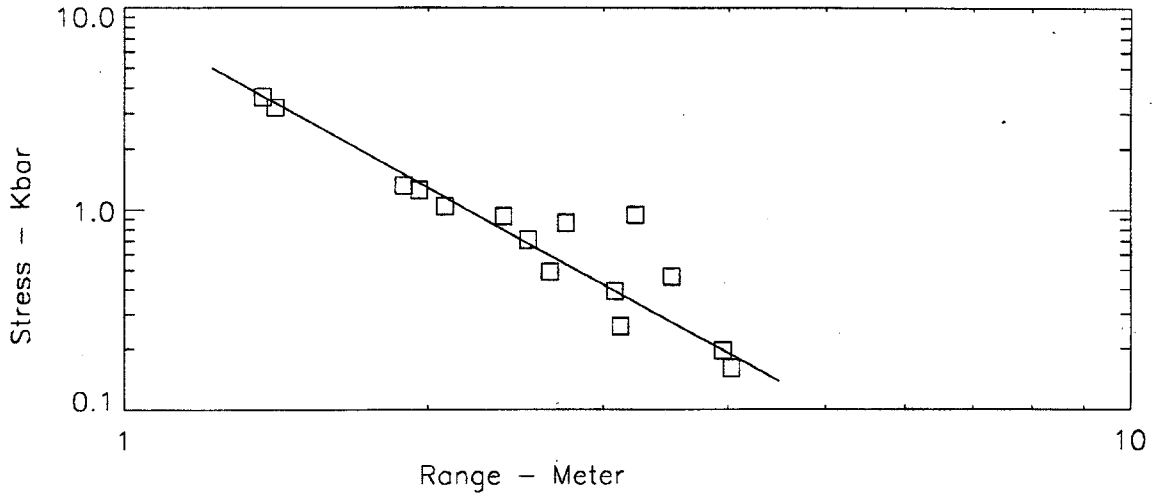

Figure 8. Peak Stress versus Range

to 40 millisecond are shown in Figure 10. Note that for clarity we have displaced the 1AYSP waveform one millisecond to the right. The decay of 1YSP is unusual. On mineback we found that, although the gage was intact electrically, the fluid cell had ruptured and thus, relieved the residual stress. By comparing 1YSP with the straight paddle 2YB at nearly the same range, we can say that

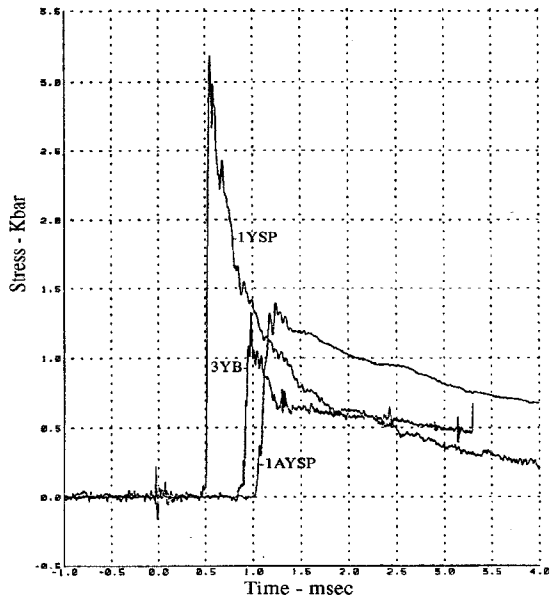

Figure 9. Traces from Two Spatula Gages and One Paddle Gage

the unloading of 1YSP is probably correct to about the 1 kbar level. Gage 2YB is shown in Figure 11. Peak stress, rise time and unloading compares well with 1YSP, thus for this stress level we see no obvious difference between a bent gage near the end of a drill hole and the usual paddle in a long

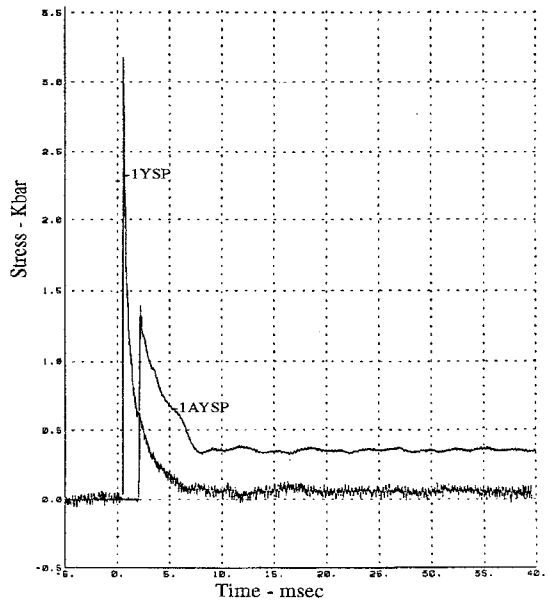

Figure 10. Traces from Two Spatula Gages

drill hole. Note the oscillations at the peak of 2YB. Often this is a sign of "clipping" by the recording equipment; here, however, the band edge was set at 4.8 kbar. Also shown in Figure 11 are traces from gages 4YB and 6YB. Gage 4YB was a thin paddle centered in a 15.2 cm (6 inch) diameter hole and grouted with GCRM. At shot time the grout had aged 9 days. At its range, it is

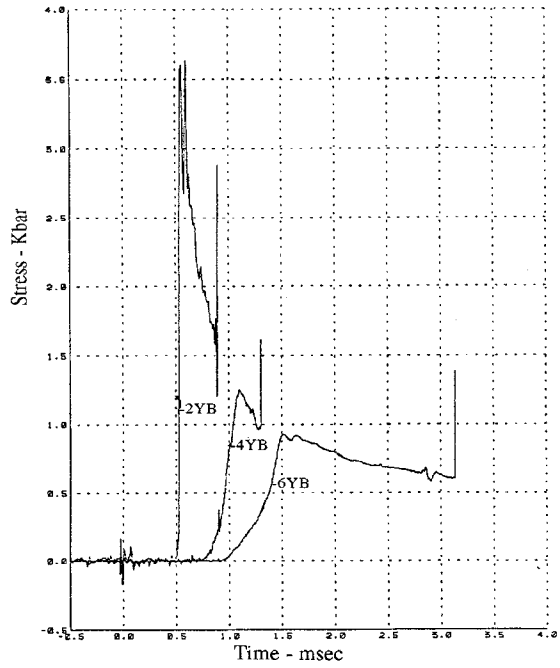

Figure 11. Traces from Ytterbium Paddles 2YB, 4YB, and 6YB

comparable with 3YB and 1AYSP (Figure 9) grouted in 10.1 cm (4 inch) diameter holes with 72-day-old GCRM. Peaks are comparable but the rise times are faster in the older grout. Also, for its range – see Figure 7 – the arrival time of the main energy of 4YB is closer to the expected arrival time than are the nearby gages 3YB and 1AYSP that were grouted with 72-day-old GCRM. The uniaxial strain tests show that the shear strength of this grout increases with age; 300 bars for 9 day-old GCRM and 400 bars for the 72 day-old material.

Also shown in Figure 11 is gage 6YB; this gage was grouted in a 10.1 cm (4 inch) diameter hole with HPNS2 grout; at shot time it had aged 78 days. The rise time of 0.5 msec is longer then the 0.35 msec rise time shown by the 5YB gage with its 72 day, GCRM grout. These aged grouts show strengths of 400 bars for the GCRM and 130 bars for the HPNS2. Thus these data suggest that stronger grout is associated with faster rise times.

Figure 12 shows waveforms from gages 5YB and 7PCR. Both were grouted with 72-day-old GCRM grout in 10.1 cm (4 inch) diameter holes. Both show oscillations at the end of the dynamic phase and the start of the residual stress regime. We can compare these traces from gages in transverse holes with those from gages (15TS) fielded in a radial, 15.2 cm (6 inch) diameter hole. All show similar oscillations. Both gages in Figure 12 show long-term offset values; gage 5YB shows 200 bars, gage 7PCR shows 100 bars. Here we have shown only 40 msec of these traces; later we show how these decayed in time.

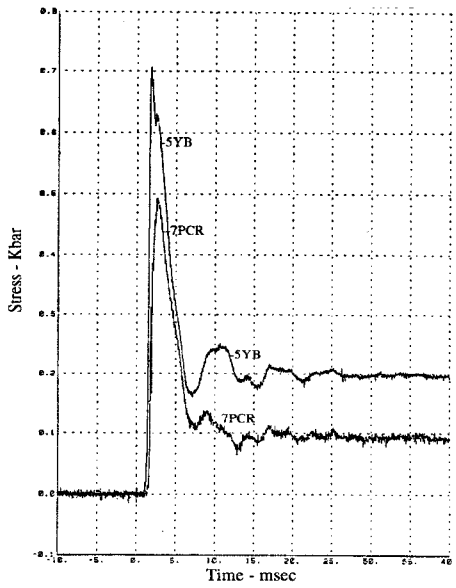

Figure 12. Traces from Ytterbium Gage 5YB and Pancake Gage 7PCR

Turning now to Figure 13 we see two ytterbium gages and the lithium niobate gage. Here we see roughly similar waveforms and three levels of peak and long-term stress. While 8YB and 11LNR were grouted in 10.1 cm holes with 72-day-old GCRM, l0YB was grouted in a slot at the end of a 20.3 cm (8 inch) hole with 9-day-old HLN(CC) grout. As discussed earlier, its peak is low. Oscillations in the 10 to 20 msec regime, for these 3 gages are similar suggesting that they are shot

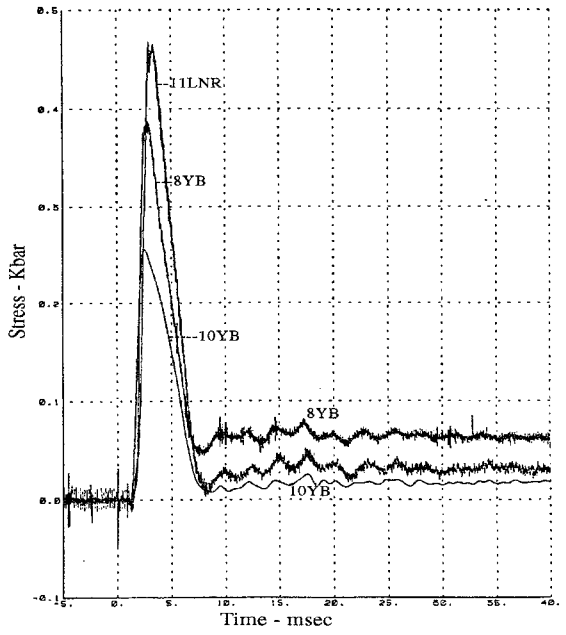

Figure 13. Traces from Ytterbium Gages 8YB and 10YB and Lithium Niobate Gage 11LNR

related and not random noise. The low residual level of 10YB in its slot compared with the gages in the round holes suggests that the round hole may contribute to the residual level. Clouding this suggestion is the additional low amplitude of the peak of 10YB, that is, what caused the low peak may also have affected the residual level. We discuss this further in the discussion of inclusion effects.

Figure 14 shows the final two ytterbium paddles fielded in 10.1 cm diameter holes. Gage 12YB was grouted with the stronger GCRM; gage 13YB was grouted with HPNS2. Both grouts aged 72 days. The peak from 13YB is approximately 80% of that from 12YB; this suggests that the stronger strength of GCRM, and lower volume compressibility compared to HPNS2, contributes to the peak amplitude. (Note, of course, that we have statistics of <u>one</u>.) The delayed arrival of the main energy for gages in GCRM grout discussed earlier is clearly seen in this figure. For 12YB the arrival of the main energy is approximately one millisecond after that for 13YB; however, 12YB clearly shows a precursor whose arrival is approximately one millisecond before the arrival shown by 13YB. Again there is a rough correspondence between the oscillations in the residual phases of 13YB and 12YB.

Figure 15 shows the traces produced by the two gages that were loaded edge-on. Gage 7PCT shows a double-peaked waveform with an amplitude of about 85 bars which is well below the radial stress value from 7PCR of 490 bars. The edge-loaded lithium niobate gage 11LNT shows an initial negative trace and then rises to a positive value of 40 bars. Pulse lengths and residual levels are notably different. Using the wave speed of 1976 m/sec from Figure 2 and the active area of these gages we can calculate the time for the wave to cross the active area. We obtain 13 microseconds for the lithium niobate and 38 microseconds for the Pancake gage. Figures 12 and 13 show that

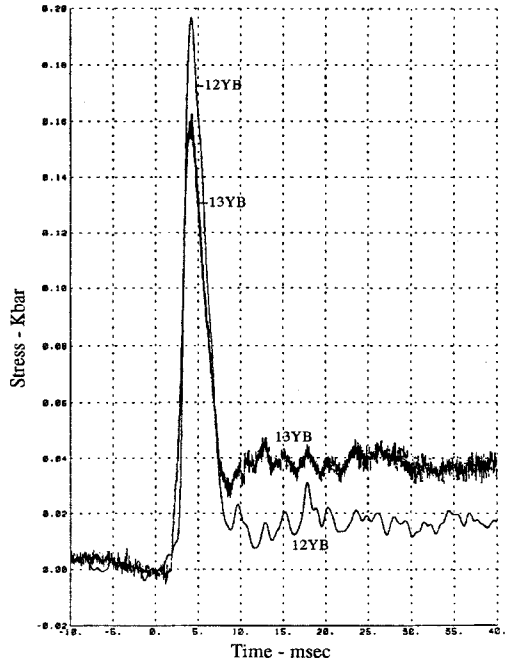

Figure 14. Traces from Ytterbium Gages 12YB and 13YB

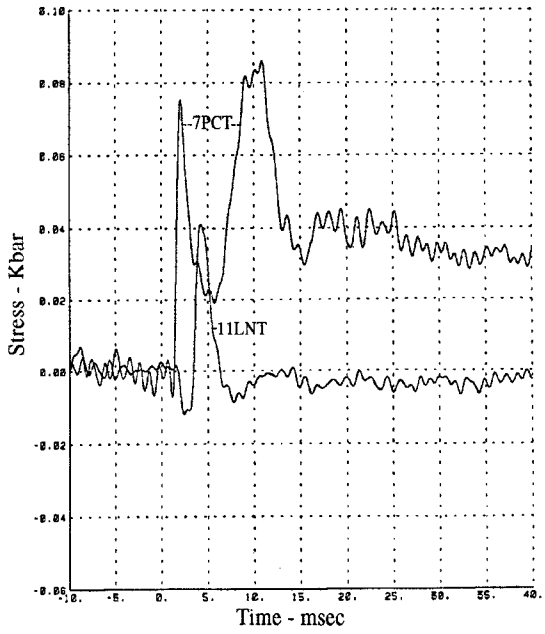

Figure 15. Traces from Edge-Loaded Gages – 7PCT and 11LNT

the risetime of the radially oriented version of these gages is about 1.5 milliseconds for the lithium niobate gage and one millisecond for the Pancake. Thus it would appear that the unusual waveform is not caused by an engulfment effect. We currently do now know how to interpret these traces. We show them as a "flag" to subsequent experimenters.

Figure 16 shows the last of the stress-time waveforms. As mentioned earlier, these gages comprised an inclusion study to compare data from gages in an epoxy cylinder grouted in a radial hole and a bare gage also in a radial hole with a calculational modeling of the configurations. Here we comment on the waveforms. The center (15TSC) and front (15TSF) gages in the epoxy cylinder show similar waveforms. The peak and residual values from the center gage are higher. Portions of the trace from the bare Toadstool grouted in the companion radial hole were obscured by a large noise pulse on that trace. In Figure 16, we see the arrival of the stress pulse and a rise to about 0.25 kbar; then at 6 msec the trace recovers and we see the oscillating residual level. (Note that in this display we have displaced the 16TS trace one msec to the right to separate the early portion from the other two traces.)

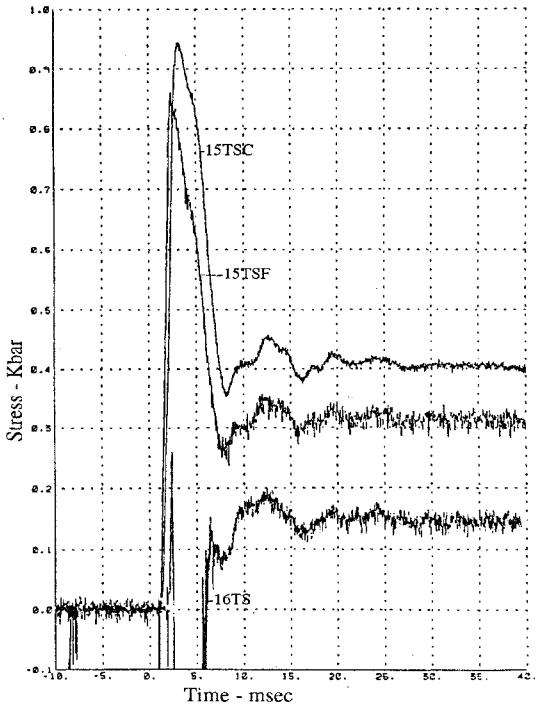

Figure 16. Traces from Toadstool Gages – 15TSF, 15TSC, and 16TS

We turn now to the acceleration measurements made on HALFTON. Table 5 gives range, time of arrival, peak acceleration and peak velocity. (Acceleration values are expressed in g where g is the standard acceleration due to gravity – 9.80 m/s^2.)

Table 5. Acceleration Measurements

Gage	Range (m)	Time of Arrival (msec)	Peak (g)	Peak Velocity (m/sec)
3AC	1.89	0.69	88,000	39
5AC	2.5	0.99	8,800	29.5
8AC	3.08	~ 1	(284)	(2.4)
12AC	3.95	1.63	450	3.9
14AG	5.68	2.47	391	2.3

Gage 8AC is notably out of agreement with the other values; in calculating least squares fits to the peak values, we excluded the 8AC data. Peak acceleration shows an attenuation of $R^{-5.1}$; peak velocity behaves as $R^{-2.85}$. These exponents may be compared with those from Perret and Bass[6]. They assembled data from three nuclear events in dry tuff; their fit to these show a decay of R to the $-(4.7 \pm 0.33)$ for acceleration and R to the $-(1.98 \pm 0.11)$ for particle velocity. The plus uncertainty gives 5.1 which is the same as our measurements.; the plus on motion gives 2.09 which is well below our 2.85. We suspect that HALFTON may have "underregistered" the motions. (The 1985 draft describes, in detail, the acceleration waveforms. Because of their low quality, these data do not appear to be worth reporting.)

Inclusion Experiments

In addition to the stress and motion gages fielded to assess wave propagation in partially saturated tuff, additional gages were fielded to examine some aspects of gage inclusion effects. This problem asks how the measurements from gages grouted in drill holes relate to the free-field measurements, that is, the stresses and motions at the gage location in the absence of the gage and grouted drill hole. For years people have assumed that with long risetimes the stress in the grout will come to equilibrium with the host rock. Not clear, however, is how a long radial hole comes to equilibrium with its host. Calculations by Swan[4] suggest that even with long risetimes there can be inclusion effects in the radial installation geometry we have used. With smaller scale experiments, such as model studies of nuclear experiments, risetimes of stress pulses may approach the transit times across the gage hole or even the whole stress pulse may be shorter than the transit time across the hole. For this case, grout properties and perhaps the shape of the inclusion – a circular hole or a slot – may affect the waveform. Of interest is the correct free-field quantity because the data is compared with a computer modeling of an event; the latter predicts the free-field quantities.

On the HALFTON event, we fielded three inclusion experiments. The first consisted of gages installed with a grout (HPNS2) that was notable more compressible than the grout (GCRM) that was used for the main gage array. The second experiment looked at inclusion geometry and size effects. One gage was grouted in a 15.2 cm (6 inch) diameter hole for comparison with a gage in a 10.1 cm (4 inch) diameter hole. Another gage was installed in a slot for a comparison with a gage in a hole. The third experiment consisted of gages in an epoxy cylinder grouted in a radial hole. In the following paragraphs we discuss these experiments.

Two gages were installed with HPNS2 grout near gages grouted with GCRM. The first comparison is between 6YB grouted with HPNS2 and 5YB grouted with GCRM. Figure 17 shows 5 milliseconds of these two waveforms. As mentioned earlier, there is a precursor before the main energy arrival on 5YB; its origin is uncertain although earlier we speculated that it may be associated with the partially saturated tuff drawing water out of the grout. The risetime of 5YB is shorter than that of 6YB; this may, however, be associated with the precursor. For 6YB the risetime is

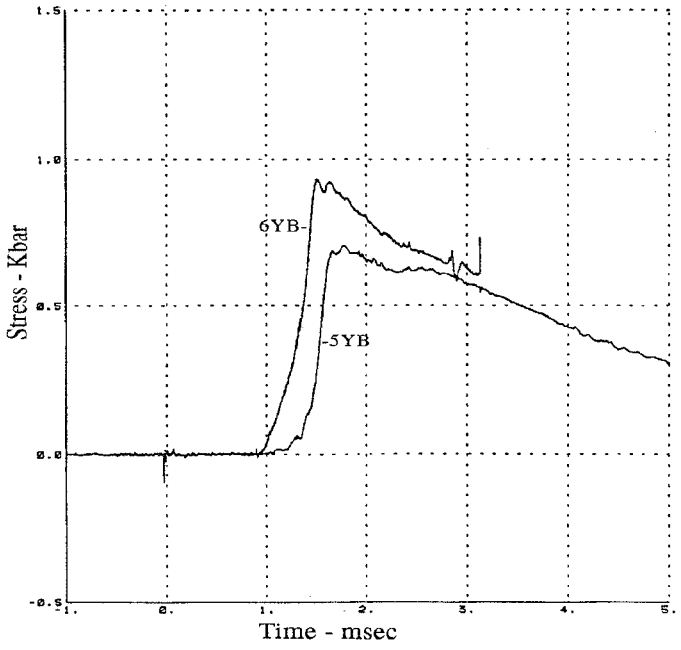

Figure 17. Traces from Ytterbium Paddles Grouted with GCRM and HPNS2

about 0.6 milliseconds. One transit across the 10.1 cm (4 inch) diameter hole takes 40 microseconds; thus the risetime represents 15 transits across the hole. With this number of transit times the grout should have come to stress equilibrium with the host rock. Gage 6YB shows a higher peak than 5YB, however, part of the difference is due to a range difference. If we assume 5YB is correct, we can evaluate what peak level we would expect at the range of 6YB. We find that the 6YB peak is 12% larger than expected for its range. An earlier figure (14) shows the comparison of the other gage pair in the two grouts – 12YB in the GCRM and 13YB in the HPNS2. Again we see the precursor on 12YB, but here, the risetimes are comparable. Range correcting the amplitude of 13YB, we find that it is 94% of 12YB which is probably within experimental error. The other notable difference is the amplitude of the residual levels. The approximate 40 bars of 13YB is twice the 20 bars amplitude of the 12YB gage. This suggests that a gage fielded in a grout (HPNS2) that is weaker than the host rock will show a higher residual level. Thus, half of the residual amplitude of 13YB may be an inclusion effect and the other half may be residual stress. In summary, the peak at the 0.75 kbar level in the HPNS2 grout is about 12% higher than in the GCRM grout, but at the 0.2 kbar level the peaks in the two grouts are comparable. Also, the weaker grout may generate an inclusion effect that is comparable to the amplitude of the residual stress.

The 3YB and 4YB gages nominally provide a comparison between gages in 10.1 cm and 15.2 cm diameter holes; however, there was also a difference in the ages of the GCRM grouts. At shot time the GCRM in the 4YB hole had aged 9 days; the GCRM in the 3YB hole had aged 72 days. The laboratory tests on this material at these two ages showed shear strengths of 400 bars for the 72-day grout and 300 bars for 9-day-old material. The volume response also differs; the older material shows slightly more compressibility. Thus the comparison provided by 3YB and 4YB is, unfortunately, more than hole size. As seen in Figure 18, peaks compare within about 5%, although their character is different. The 1.1 kbar shoulder on 3YB and subsequent 1.32 kbar peak suggest we are seeing reverberation in the 10.1 cm hole, that is, the 1.1 kbar peak may be the impedance match peak between the tuff and the grout, and the subsequent peak is the reflection from the back side of the hole. (The transit time across the hole is about 31 microseconds. The spiky nature of the

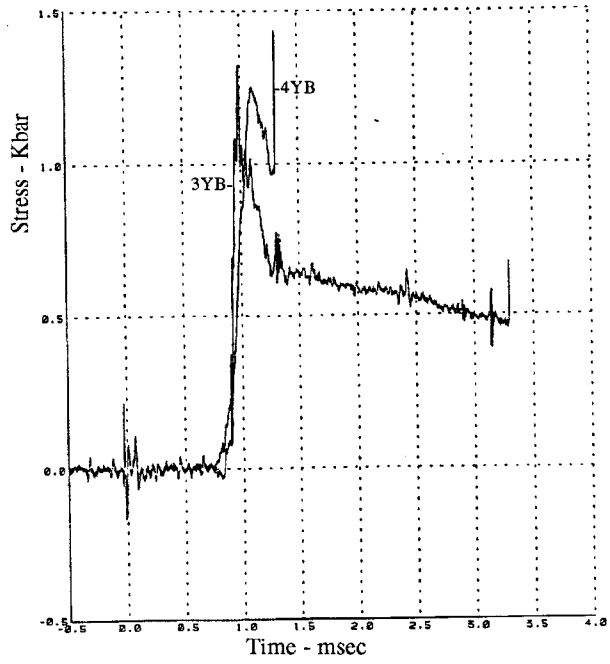

Figure 18. Traces from Ytterbium Paddles with Varying Hole Sizes and Grout Ages

waveform, however, may also have been generated by reverberations in the gage package. In contrast, 4YB in the 15 cm hole has a much smoother peak. The risetimes of the two waveforms also differ by a factor of three. Gage 4YB emerges from the noise and smoothly rises in about 300 microseconds to its peak. The gage in the older grout shows an approximately 100 microsecond long precursor before rapidly rising. In summary, the 1.5 times greater diameter hole for 4YB versus 3YB would not seem to explain the 3X increase of risetime of 3YB over 4YB. The difference would appear to be associated with the age related, increased strength of the grout.

The second geometry effect was a gage installed in a slot and its comparison with a gage in a hole. The earlier Figure 13 shows the comparison of 8YB in the 10.1 cm diameter hole and 10YB in the slot. Two notable differences are seen: the 10YB peak amplitude is two thirds of the peak from 8YB and there is about a 3X difference in residual levels. Intuition, based on shock wave knowl-

edge, suggests that a gage in a slot should rapidly come to stress equilibrium with the host. Also, a gage grouted in a hole with a grout that is a good material property match to the host has been shown by calculations to reflect the stress in the host, thus the major difference in peak response is surprising. Different grouts were used for these gages. Gage 8YB was grouted with GCRM and was about 75 days old at shot time. The gage in the slot was grouted with HLN(CC) which had aged 9 days at shot time. We needed to use a less viscous grout than GCRM for the slot; our fear was that, if we used the GCRM in the slot, we may not have filled the slot. Previous experience suggests that an air void near a stress gage notably affects the stress field. Laboratory tests on these two grouts, however, show that 9 day-old HLN(CC) and 75-day-old GCRM show comparable (330 vs. 344 bar) unconfined crush strengths. This suggests that their shear strengths are similar.

Another item that may have affected the response of the slot gage was the presence of a drill hole used in cutting the slot. Figure 19 shows two views of the gage and slot. The slot was cut at the end of a 20.3 cm diameter drill hole. (This was not a trivial task.) The sensing portion of the gage was 18.3 cm from the end of the drill hole. Also note that the slot is offset from the axis of the hole. There may have been a shadowing effect or perturbation of the waveform that affect the amplitude of the signal. A perturbation off the corner of the grouted hole would arrive about 50 microseconds after the direct arrival. With a risetime of 500 microseconds for 10YB, the perturbation could have affected the peak. In summary, the major effort to cut a slot and install a gage in a geometry that promised rapid equilibrium with the host may have been affected by the presence of the drill hole.

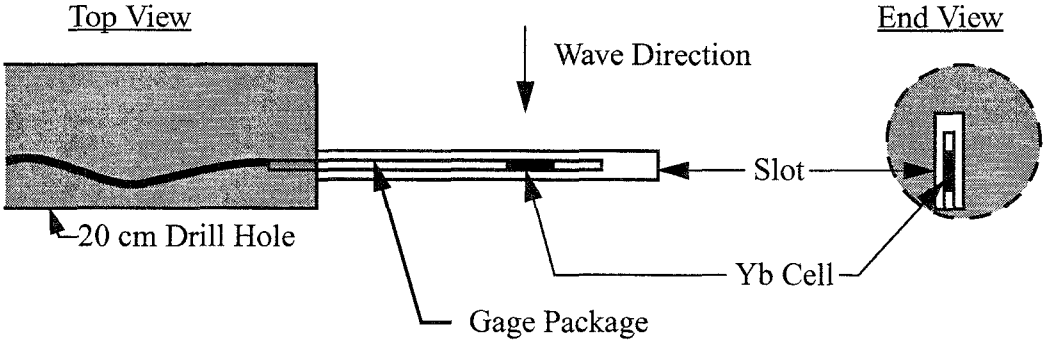

Figure 19. Two Views of Slot Installation Geometry

The third inclusion experiment involved gages encapsulated in epoxy cylinders and grouted in holes radial to the work point. This is the arrangement typically used on nuclear events; we wanted to know if there was an inclusion effect in this experimental arrangement. Earlier static calculations by Pacifica Technology[7] showed that the stress amplitude declined from its free-field value to a lower value in the grout in front of the gage package and then rose to about twice the free-field value in the epoxy cylinder. Figure 20 shows a sketch of the variation of radial stress along the axis of the hole in the presence of the grout and epoxy cylinder. The effect of the approximately twice free-field stress in the center of the epoxy cylinder was shown by Pacifica Technology to be related to the high strength of the epoxy compared to the strengths of the tuff and grout. Gages

Figure 20. Behavior of Static Stress in Presence of Grouted Drill Hole

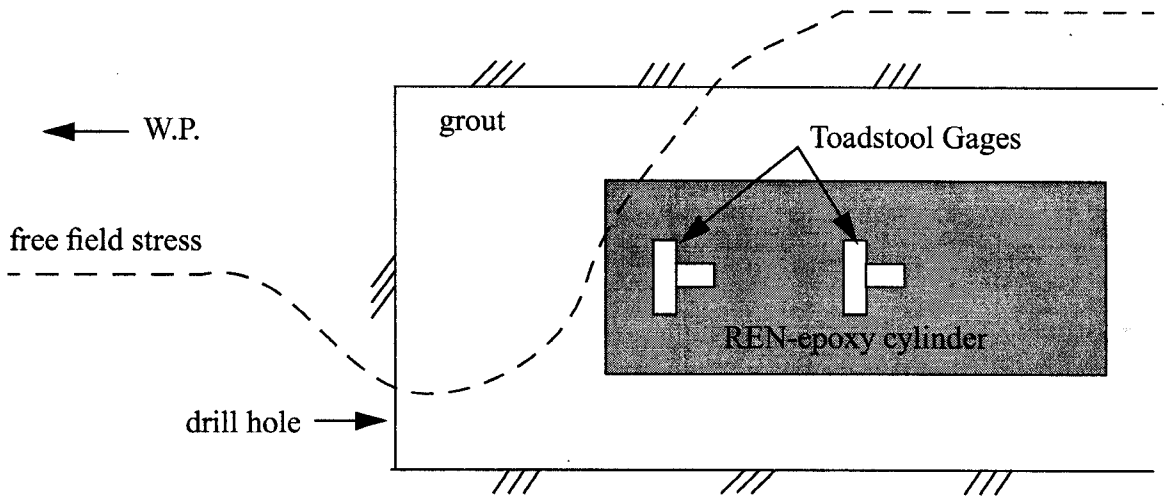

15TSF, 15TSC and 16TS were designed to provide measurements on this effect. Gages were fielded in nearly radial holes with the grout (HPNS2) that is usually in radial holes on nuclear events. Hole 16 contained a "bare" Toadstool gage; hole 15 contained an epoxy cylinder with a Toadstool gage located near the work point end (15TSF) and a Toadstool located near the center of the cylinder (15TSC). The earlier Figure 16 shows the waveforms measured by these three gages. As mentioned earlier, an unfortunate noise burst obscured the dynamic portion of gage 16TS; we see the wave arrival and the latter residual portion of the waveform. The 15TS gages show a higher stress from the center gage – as suggested by the static calculation – and a larger residual level from the center gage. Comparing the peaks from the 15TS gages with peaks from gages in the tangential holes – Figure 8 – we see them to be well above the peaks from the other gages suggesting an inclusion effect.

Swan at Pacifica Technology performed a dynamic calculation on the radial hole, epoxy cylinder configuration. Figure 21 shows a modified version of a figure in Swan's report[4]. Here we see his calculation of the free-field stress and the calculated stress in the REN epoxy at the two gage ranges. Also plotted are the field measurements. At 2.72 meters – the range for 15TSF – we see a calculated free-field peak of 0.63 kbar, a calculated inclusion peak of 0.85 kbar and a measured peak of 0.9 kbar. At the 3.24 meter--the range for 15TSC--we see a calculated free-field stress of 0.37 kbar, a calculated inclusion peak of 1 kbar and a measured peak of 1 kbar. At the front location the calculated inclusion peak is 1.3 times the free field; at the center location the inclusion peak is 2.7 times the free field. At the front location the measured peak lies above the predicted free field and inclusion peaks. At the center location the measurement agrees with the predicted inclusion peak. What is missing here is a measurement of the actual free-field stress; with it one could validate the calculation and allow a quantitative comparison between the measurements and calculations. Note, however, that the calculated free-field stress at 2.72 meters of 0.63 kbar is 1.2 times the 0.54 kbar peak obtained from extrapolating from gages in tangential holes. At the 3.24 m range the free-field calculation is 0.37 kbar; the stress peak extrapolated from the tangential gages measurements is 92% of that value (0.34 kbar). Thus we see sufficient agreement between the calculational modeling and the measurements to suggest that the modeling is valid.

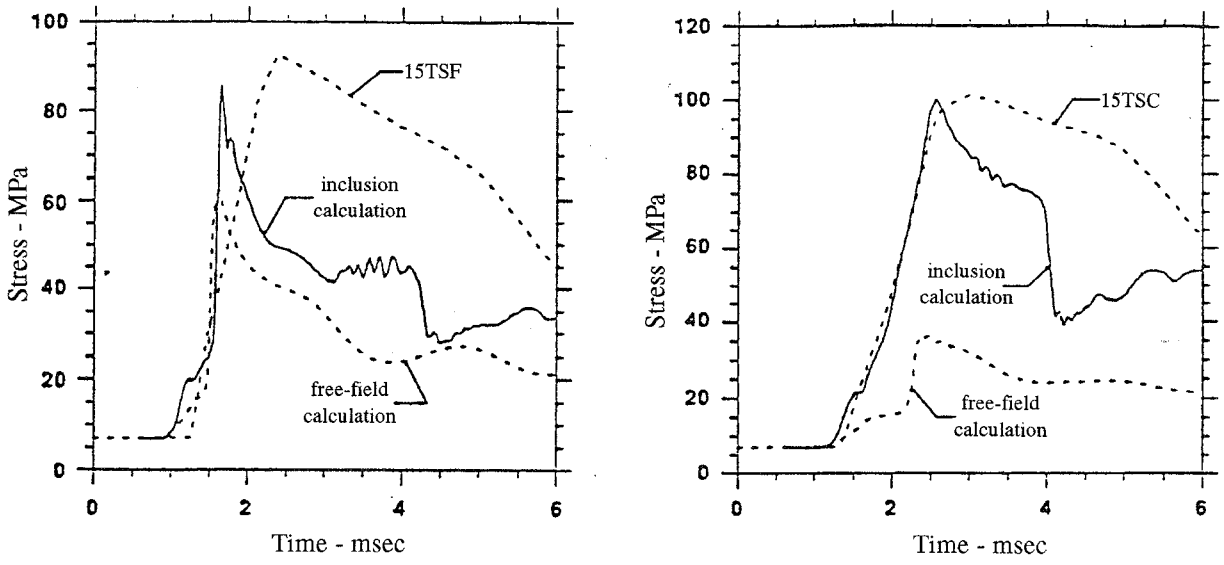

Figure 21. Comparison of Calculations and Data for REN Gage Configurations

In the residual phase, gages 15TSF, 15TSC, and 16TS show notably different amplitudes; see Figure 16. Gage 16TS without the epoxy cylinder shows the lowest value of 150 bars, the front gage in the epoxy shows about 300 bars, and the center gage shows 400 bars. While we can not show that there are inclusion effects for the bare gage, we can infer by the amplitude differences that the gages in the epoxy cylinder are showing inclusion effects.

In summary, static and dynamic calculations predict an inclusion effect for gages encapsulated in epoxy cylinders and grouted in radial holes; measurements qualitatively confirm these calculations. (At this point the 1985 draft describes and shows data on the recorded late-time measurements. The 1996 view is that these data are "tainted" by inclusion effects. A motivated reader, however, may access the original draft, and the data, in the Sandia TIP files.)

Mineback

Mineback on HALFTON proceeded in the tuff to the right of the grouted access drift. Mine-back objectives were:

Examine size and shape of the cavity
Recover SEA and LLNL experiments
Recover gages and examine grout-tuff interfaces

The HALFTON cavity showed a high degree of symmetry about the work point. Departures from the uniform surface were associated with the add-on experiments – the LLNL "rock box" and the SEA cavity pressure hardware. In the horizontal plane the radii varied from 1.0 to 1.16 meters. An average of 19 equally spaced horizontal radii was 1.07 meters (3.52 ft.). The normal "onion" skin zone of crushed rock surrounded the cavity and was 0.46 meters in thickness. Occasional radial

fractures were seen in the onion skin zone; very few extended beyond the onion skin zone. Where radial fractures did extend, they existed as slippage planes which can be seen where they crossed grouted instrument holes and gages. Recovered gage 2YB showed this effect; it was probably the cause of the 2YB record ending at 0.9 milliseconds. Radial fractures containing black detonation products extended into the grout stemming plug; however, some of these were associated with the SEA spiral cavity gage. None of the radial fractures extending into the tuff contained detonation products.

One cavity pressure pipe (CP1) extended about 10 cm into the cavity; the tip of the second (CP2) was in the grout stemming about 10 cm from the cavity wall. Initially, the pipe tips were 0.46 and 0.61 meters from the surface of the high explosive; both moved 0.14 meters. During the dynamic phase, one cavity pressure pipe broke at a location outside the stemming. This allowed the pressure in the cavity to unload. The unloading, however, was slow enough that the remaining amplitude pressurized the SEA spiral pipe and drove pressure into the LLNL cable.

Gages were recovered and breaks were noted. Photographs taken during the recovery process showed that the sensing element for gage 10YB was 30.0 cm (11.8 in.) into the slot from the 20 cm (8 inch) diameter insertion hole. With one exception, the grout filled the holes and showed intimate contact with gage packages and the tuff host rock. The exception was seen on instrument hole number 12 where there was a half to one centimeter diameter air pocket at the interface of the accelerometer package and the ytterbium paddle. Also, there was a thin layer – perhaps 2mm thick – of a friable grout material at the crown of the number 12 hole. Between this altered material and the gage package was a minimum of about one centimeter of normal GCRM grout.

In summary mineback showed that the detonation produced a symmetric cavity with a 1.07 meter radius. A few radial fractures were seen; at least one sheared a gage. Except for one small air pocket, we found intimate contact between gages, grout and the tuff host.

Conclusions

HALFTON was one event of a series of nuclear containment-related experiments in which a 453 kg high explosive charge was detonated in the ashfall tuff of G Tunnel at the Nevada Test Site. We fielded instruments to measure stress and motion to explore the phenomena of a contained detonation in this 90% water saturated tuff. A mined entry (mineback) into the cavity postevent allowed us to assess the cavity size and shape, recover gages and passive experiments. Ytterbium stress gages fielded at ranges from 1.4 to 5.7 m measured the dynamic stress waveforms; peak decay shows a behavior of range raised to the -2.77 power. A limited number of stress gages were also fielded to explore gage inclusion effects. Some measurements agreed qualitatively with computer modeling, others disagreed.

On mineback we found the cavity to be nearly circular in the horizontal plane with an average radius of 1.07 meters. Intimate contact between gage packages, grout, and host rock was seen. Failure modes of gages and cables were also observed.

References

1. C. W. Smith, *PUFF TOO: A Residual Stress Experiment*, SAND79-1674. Sandia National Laboratories, Albuquerque, NM, April 1980.

2. G. Torres and W. Klauber, *Material Characterization of NTS Tuff from U12g. RS#19 GH#3*, TR 86-60R, TerraTek Research, Salt Lake City, UT, January 1986.

3. J. Lupo, et al, *Physical and Mechanical Characterization of Tuff from U12g. RS#19 IH#2, IH#4 and IH#5, and GCRM Grouts, HALFTON Event.* TR 87-01, TerraTek Research, Salt Lake City, UT, August 1986.

4. C. C. Swan and C. W. Smith, Theoretical and Experimental Analysis of In-Situ Gauge Inclusion Effects, in Proceedings of the *Fourth Symposium on Containment of Underground Nuclear Explosions - Volume 1, Sept 1087, United States Air Force Academy, Colorado Springs, CO.*

5. B. A. Hartenbaum, *The Design of Subterranean Instrumentation Cables to Survive Large Amplitude Ground Motions*, DNA 4636F, H-Tech Laboratories, Inc. Santa Monica, CA, July 1978.

6. W. R. Perret and R. C. Bass, *Free-Field Ground Motion Induced by Underground Explosions*, SAND74-0252, Sandia National Laboratories, Albuquerque, NM, February 1975.

7. C. C. Swan and D. F. Patch, *Equilibrium Analysis of Axially loaded Cylindrical Inclusions*, DNA-TR-86-346, Pacifica Technology, Del Mar, CA, May 1986.

DISTRIBUTION:

Dr. N. R. Burkhart, L-221
Lawrence Livermore National Laboratory
P.O. Box 808
Livermore, CA 94550

Dr. F. N. App, F659
Los Alamos National Laboratory
P.O. Box 1663
Los Alamos, NM 87543

Dr. W. M. Brunish, F659
Los Alamos National Laboratory
P.O. Box 1663
Los Alamos, NM 87543

FCDNA/FCTT
attn: B. Ristvet
1680 Texas St.
Kirtland AFB, NM 87117

FCDNA/FCTO
attn: M. O'Brien
1680 Texas St.
Kirtland AFB, NM 87117

Dr. E. Peterson
S-Cubed
P.O. Box 1620
La Jolla, CA 92038

Dr. N. Rimer
S-Cubed
P.O. Box 1620
La Jolla, CA 92038

Dr. D. Patch
SAIC/PacTec Division
10260 Campus Point Dr., M/SC2
San Diego, CA 92121

Dr. A. Florence
SRI International
333 Ravenswood Ave.
Menlo Park, CA 94025

Paul DeCarli
SRI International
333 Ravenswood Ave.
Menlo Park, CA 94025

Robert Bass
7705 Cedar Canyon Pl. NE
Albuquerque, NM 87122

MS 1160 T. K. Bergstresser
MS 1160 H. D. Garbin
MS 1160 K. Glibert
MS 1160 J. D. Plimpton
MS 1160 J. R. Banister
MS 1160 C. W. Smith (5)
MS 1159 J. I. Greenwoll
MS 1159 E. Vieth
MS 1170 P. Nelson
MS 1391 R. C. Shear
MS 0821 M. D. Furnish
MS 0821 D. E. Grady

MS 9018 Central Technical Files, 8523-2
MS 0899 Technical Library, 4414 (5)
MS 0619 Print Media, 12615
MS 0100 Document Processing, 7613-2
for DOE/OSTI (2)